Experimental investigation on micromilling of oxygen-free, high-conductivity copper using tungsten carbide, chemistry vapour deposition, and single-crystal diamond micro tools

D Huo[1]* and **K Cheng**[2]
[1]Product Design and Engineering Department, Middlesex University, London, UK
[2]Advanced Manufacturing and Enterprise Engineering Department, Brunel University, Uxbridge, UK

Abstract: Insufficient experimental data from various micro tools limit industrial application of the micromilling process. This paper presents an experimental comparative investigation into micromilling of oxygen-free, high-conductivity copper using tungsten carbide (WC), chemistry vapour deposition (CVD) diamond, and single-crystal diamond micromilling tools at a uniform 0.4 mm diameter. The experiments were carried out on an ultra-precision micromilling machine that features high dynamic accurate performance, so that the dynamic effect of the machine tool itself on the cutting process can be reduced to a minimum. Micromachined surface roughness and burr height were characterized using white light interferometry, a scanning electron microscope (SEM), and a precision surface profiler. The influence of variation of cutting parameters, including cutting speeds, feedrate, and axial depth of cut, on surface roughness and burr formation were analysed. The experimental results show that there exists an optimum feedrate at which best surface roughness can be achieved. Optical quality surface roughness can be achieved with CVD and natural diamond tools by carefully selecting machining conditions, and surface roughness, R_a, of the order of 10 nm can also be obtained when using micromilling using WC tools on the precision micromilling machine.

Keywords: micromilling, micromachining, OFHC copper, single-crystal diamond tools, tungsten carbide, CVD diamond, micromachinability

1   INTRODUCTION

High-accuracy miniature components with dimensions ranging from a few hundred micrometres to a few millimetres, or features ranging from a few to a few hundred micrometres, are increasingly in demand for industries such as electro-optics, automotive, biotechnology, aerospace, medical, and information and communications technology [1–3]. Some miniature or microcomponents require complex, three-dimensional (3D) geometries and need to be made from a va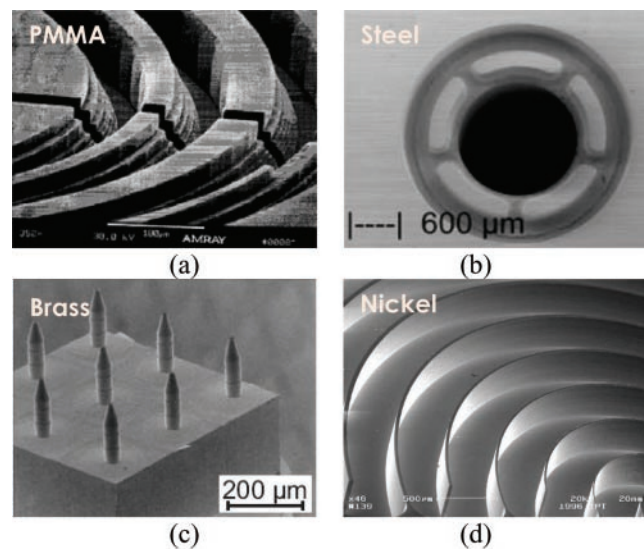riety of engineering materials. The materials are application-dependent, optical components made from glass, polymer, or aluminium, medical components from polymer or glass, mechanical components from ferrous or non-ferrous metals, and dies/moulds from copper alloys, aluminium, or high-hardness steels [4–12]. In some particular applications, microcomponents and microstructures even require submicrometre accuracy and nanometre surface roughness [13]. It has long been recognized that traditional MEMS manufacturing techniques, such as chemical etching and LIGA, are not suitable for producing true three-dimensional (3D) micro components [8, 14]. Mechanical micromachining is, however, an ideal method to produce high-accuracy microcomponents in various engineering materials. Among several mechanical machining processes, micromilling is the most flexible and productive process and

Corresponding author: Product Design and Engineering Department, School of Engineering and Information Sciences, Middlesex University, Bramley Road, London N14 4YZ, UK. email: d.huo@mdx.ac.uk

thus is able to generate a wider variety of complex microcomponents and microstructures at small and medium lot size in particular. Some examples of high-accuracy, micromilled components and micro-structures [4–7] are illustrated in Fig. 1.

There are numerous cutting-tool materials being used in conventional machining processes, and the properties of these materials vary in terms of hardness, toughness, wear resistance, etc. However, only a few tool materials have been used for fabricating micromilling tools. Tungsten carbide (WC) is a popular tool material widely used in micromachining processes. There are some micromilling experimental data on using WC tools available in the literature [15–17], but data recommended by tool manu-facturers cannot normally be applied to micromilling directly. In addition, some micromilling models based on WC tools have been proposed in the past five years [16–19].

Coated micro tools, i.e. chemistry vapour deposi-tion (CVD) diamond or CBN coatings, are used in some applications to elongate tool life [20]. However, the thickness of the coatings would significantly increase the cutting edge radius by a few micro-metres [21] and thus blunt the tool, although this might not be an issue for macro-scale cutting tools. In micromachining, however, the depth of cut is in the range of a few micrometres, and typical features of the microcomponent are in the range of tens to hundreds of micrometres; the well-known size effects will thus play a significant role and change the whole machining process physics. Therefore, increasing the cutting edge radius owing to coatings will nega-tively affect the micromachining performance [21],

although they have a positive effect in terms of wear resistance and low cutting friction. More experi-mental results are expected to assess the coated microtool performance.

Single-crystal diamond and CVD diamond micro-milling tools have been introduced to micromachin-ing in recent years. Single-crystal diamond or CVD diamond micromilling tools have the potential of achieving high-dimensional/form accuracy and an optical surface roughness in various engineering materials, because they not only offer exceptional hardness but also have a submicrometre-level cutting edge radius (typically 1–5 μm for WC and coated microtools). Up to now, almost no micromilling data related to single-crystal diamond and CVD diamond microtools have been reported. Insufficient micro-milling experimental data are limiting industrial application of micromilling and the understanding of surface and burr formation under various cutting conditions.

Most of the micromilling experiments reported in the literature were performed in miniature machine tools (MMTs) [22–26] or conventional machining centres with retrofitted high-speed spindles [11, 15, 21], which have limited stiffness or accuracy, and results may not be industrially applicable. Therefore, optimum cutting conditions from various micro-milling tools, obtained directly from industrial-precision micromilling machines rather than MMTs and test beds, are desirable for micromachining, so as to bridge the gap.

In this paper, an experimental comparative inves-tigation into micromilling of oxygen-free, high-conductivity (OFHC) copper using WC, CVD dia-mond, and single-crystal diamond milling tools is presented. The experiments were performed on an ultra-precision micromilling machine to minimize the effect of the machine tool itself on the micro-machining performance. The influence of variation of cutting parameters, including cutting speeds, feedrate, and depth of cut, on surface roughness and burr formation was analysed.

Fig. 1 Examples of high-accuracy micromilled compo-nents and microstructures: (a) micro trenches [4]; (b) micro mould [5]; (c) micro needles array [6]; (d) micro wall [7]

2 EXPERIMENTAL SET-UP AND PROCEDURES

2.1 Ultra-precision micromilling machine: UltraMill

Experiments for this work were carried out on a five-axis ultra-precision bench-top micromachine, Ultra-Mill, which was developed by the authors at Brunel University (see Fig. 2). The UltraMill is a general-purpose, ultra-precision micromachine with three linear axes and two rotary axes. The five-axis config-uration offers maximum flexibility in tool–workpiece orientation and minimum need for re-set-up, which

is important to achieve high accuracy on micro parts. Although it is designed for micromachining micro parts, a relatively large machining envelope of $150 \times 150 \times 80\,mm^3$ was specified to enable it to machine large-size components with micro features. The overall footprint is about $1\,m^2$ including the periphery, which is only 10–20 per cent of that required by conventional ultra-precision machines.

Aerostatic bearings are employed in the machine tool throughout, which differs from most of the ultra-precision machine tools on the market. Three linear slides are driven by ironless, brushless linear motors, and the rotary table is driven by a direct-drive torque motor. In order to improve dynamic stiffness of the aerostatic bearing, a novel squeezed oil film damper is fitted to all slides, and the rotary table in the machine tool developed. Therefore, sub micrometre machining accuracy under dynamic cutting force conditions is guaranteed by the above technologies. The extremely smooth and accurate motion provided by aerostatic bearings, along with diamond tooling, also makes nanometre-range surface roughness on microcomponents possible.

The machine is equipped with a high-speed air bearing spindle that is driven by a DC brushless motor. The spindle developed is 63 mm in diameter and 115 mm in length and weighs 2.5 kg, with a 3 mm

precision four-jawed collet. It has a maximum speed in excess of 200 000 r/min, a radial runout of less than $2\,\mu m$, and a radial stiffness of 3 N/m measured at the collet end. Bearing friction losses are less than 50 W at maximum speed, but even so, water cooling is used to minimize thermal distortion [2].
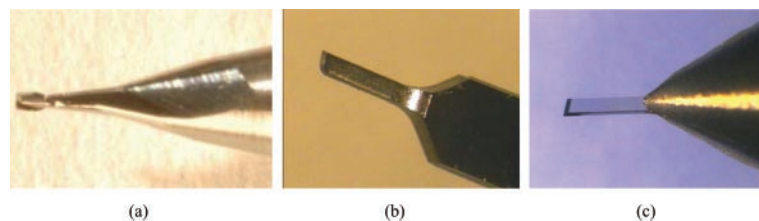
2.2 Micromilling tools

The micromilling tools used in the experiments include two-fluted WC end-mills, one-fluted CVD diamond microtools, and one-fluted single-crystal diamond microtools. CVD diamond micromilling tools were fabricated using laser machining, and single-crystal diamond milling tools were fabricated using mechanical grinding and polishing. CVD diamond tools can achieve similar machining quality to that of single-crystal diamond tooling in terms of accuracy and surface finish, and also have the advantage of machining ferrous materials that cannot be processed by single-crystal diamond tooling. Unfortunately, there are almost no CVD and single-crystal diamond micromilling data available in the literature. All micromilling tools have a nominal diameter of 0.4 mm and are capable of full immersion slot milling. A uniform tool shank diameter of 3 mm is used for all micro tools to fit the 3 mm precision spindle collet. Figure 3 shows the three types of micromilling tool used for the experiments.

2.3 Procedure and cutting conditions

The experiments in this work include full immersion slot milling, as illustrated in Fig. 4. For each test, a micro slot 4 mm long and 0.4 mm wide was milled along the y-direction. OFHC copper was chosen as the workpiece material in this work because it has excellent machinability for both WC and diamond tools, and it is widely used in the optics and mould industries. Before experiments, the top surface of the workpiece was prepared using a 2 mm end-mill. A small axial depth of cut of 5 μm at each pass was used for the surface preparation to eliminate surface damage. A machine vision system (InfiniStix™ microscope) is integrated into the machine tool, providing 3 μm resolution in the z-direction to assist in positioning the cutter to the workpiece surface.

Fig. 2 The UltraMill – ultra-precision micromilling machine: (a) WC; (b) CVD diamond; (c) single-crystal diamond

Fig. 3 Micromilling tools used in the experiments (*courtesy of Contour Fine Tooling Limited*)

The feed per tooth F_z was varied at 0.1μm, 0.2 μm, 0.5 μm, 1 μm, 2 μm, 3 μm, and 4μm, respectively, at a constant axial depth of cut of 30 μm. The wide range of feedrate was chosen to ensure that minimum chip thickness for all three cutters and workpiece combinations falls into this range, so that the size effect due to the minimum chip thickness can be investigated. The spindle speed n was varied at 10 000, 30 000, 60 000, and 90 000 r/min, respectively, during these experiments. Effect of axial depth of cut d was also studied by varying its value from 10 μm to 100 μm at intervals of 10 μm, and fixing the spindle speed at 60 000 r/min. Oil-based coolant mist was sprayed onto the cutting zone during all of the micromilling experiments. The aforementioned experiments were
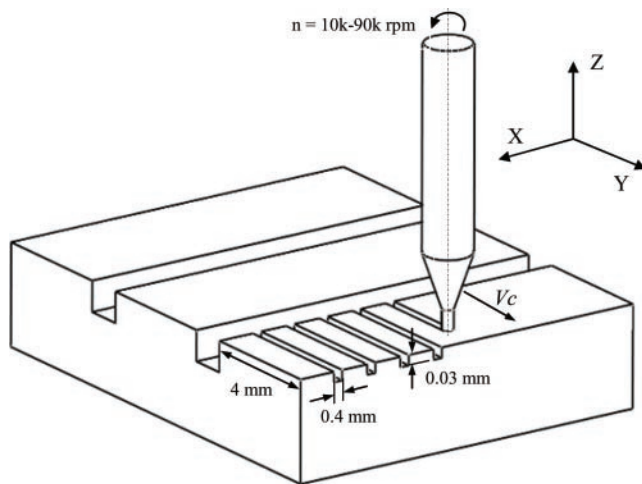

Fig. 4 Schematic diagram of the micromilling experiment

repeated on all three types of micro tool. The full experimental matrix is listed in Table 1.

In order to reduce the influence of tool wear on the surface and burr formation, brand new micro tools were used for each set of experiments. An extra slot (experiment 39) was milled at the end of the experiments using the same cutting conditions as for the first slot (see Table 1). This validation slot was then compared with the first slot (experiment 1). For the three types of micro tool, it is observed that there is no significant difference between experiments 1 and 39 in terms of surface roughness, slot width, and burr height. Therefore, the tool wear effect is regarded as negligible for the cutting distance used in this work.

2.4 Surface roughness and burr height measurement

The surface roughness of the bottom surface of the micromilled slots was measured using a white light interferometer (Zygo NewView 5000) along the centreline of the slots. To reduce the measurement uncertainty and assess repeatability, five measurements on different areas were conducted for each slot, and an average value of surface roughness (R_a) was used for analysis. There is no standard method of evaluating burr formation. In this research, an average burr height measured across the slot was used quantitatively to assess burr formation. Five measurements of burr height were recorded using a surface profiler (Talysurf Serial-2), and an average value was calculated for discussion.

Table 1 Experimental matrix for micromilling using WC, CVD, and single-crystal diamond milling tools

Experiment no.	Depth of cut, d (mm)	Spindle speed, n (r/min)	Cutting speed, V_c (m/min)	Feedrate, F_z (μm/flute)	Experiment no.	Depth of cut, d (mm)	Spindle speed, n (r/min)	Cutting speed, V_c (m/min)	Feedrate, F_z (μm/flute)
1	0.03	10 000	12.56	0.1	21	0.03	60 000	75.36	4
2	0.03	10 000	12.56	0.2	22	0.03	90 000	113.04	0.1
3	0.03	10 000	12.56	0.5	23	0.03	90 000	113.04	0.2
4	0.03	10 000	12.56	1	24	0.03	90 000	113.04	0.5
5	0.03	10 000	12.56	2	25	0.03	90 000	113.04	1
6	0.03	10 000	12.56	3	26	0.03	90 000	113.04	2
7	0.03	10 000	12.56	4	27	0.03	90 000	113.04	3
8	0.03	30 000	37.68	0.1	28	0.03	90 000	113.04	4
9	0.03	30 000	37.68	0.2	29	0.01	60 000	75.36	0.5
10	0.03	30 000	37.68	0.5	30	0.02	60 000	75.36	0.5
11	0.03	30 000	37.68	1	31	0.03	60 000	75.36	0.5
12	0.03	30 000	37.68	2	32	0.04	60 000	75.36	0.5
13	0.03	30 000	37.68	3	33	0.05	60 000	75.36	0.5
14	0.03	30 000	37.68	4	34	0.06	60 000	75.36	0.5
15	0.03	60 000	75.36	0.1	35	0.07	60 000	75.36	0.5
16	0.03	60 000	75.36	0.2	36	0.08	60 000	75.36	0.5
17	0.03	60 000	75.36	0.5	37	0.09	60 000	75.36	0.5
18	0.03	60 000	75.36	1	38	0.1	60 000	75.36	0.5
19	0.03	60 000	75.36	2	39	0.03	10 000	12.56	0.1
20	0.03	60 000	75.36	3					

3 RESULTS AND DISCUSSIONS

This section presents the experimental results and the associated discussions. First, surface roughness results obtained from the three types of micro tool are discussed, followed by the burr formation discussion.

3.1 Surface roughness

Figure 5 shows average surface roughness R_a as a function of feedrate at various cutting speeds for the three types of micromilling tool. It can be observed from Figs 5(b) and (c) that, for CVD and single-crystal diamond micro tools, the tendency is towards higher roughness values with increases in feedrate when the feedrate is greater than 0.5 μm/tooth. However, when the feedrate is smaller than 0.5 μm/tooth, the roughness value decreases with increases in feedrate. The smallest surface roughness for single-crystal diamond tools is observed around 11 nm, occurring at 0.2 μm/tooth, and a cutting speed of 12.56 m/min; the smallest surface roughness for CVD diamond tools is observed around 13 nm, occurring at 0.2 μm/tooth, and a cutting speed of 37.68 m/min. The good surface roughness obtained from micromilling using CVD and single-crystal diamond tools indicates that an optical surface roughness can be achieved in micromilling by carefully selecting cutting conditions.

The tendency of surface roughness results for WC tools is towards a lower roughness value with an increase in feedrate, until the feedrate exceeds 3 μm/tooth (see Fig. 5(a)), which is different from that of CVD and single-crystal diamond tools. Under the cutting conditions in this work, a surface roughness, R_a, between 24 and 50 nm was achieved. The smallest R_a value of 24 nm was observed at a feedrate of 3 μm/tooth and a cutting speed of 75.36 m/min. It should be noted that the surface roughness results and the smallest R_a value of 24 nm achieved in this work are much better than some micromilling data obtained from miniature micromachine tools in the literature. This indicates that the micromilled surface roughness depends, not only on the cutting tools and cutting conditions, but also on the whole machining system, including the motion errors of slideways and spindle runout, etc.

Generally, for all three types of micro tool, spindle speed has no significant effect on the surface roughness. However, for CVD and single-diamond tools, cutting speeds have a negative effect on the surface, i.e. the higher the cutting speed, the higher the surface roughness value, especially for higher cutting speeds (see Figs 5(b) and (c)). By contrast, this trend has not been found in WC micromilling experiments.

When the feed per tooth (i.e. depth of cut) is of the same order as the tool edge radius, the effective rake angle may become negative. Size effects resulting
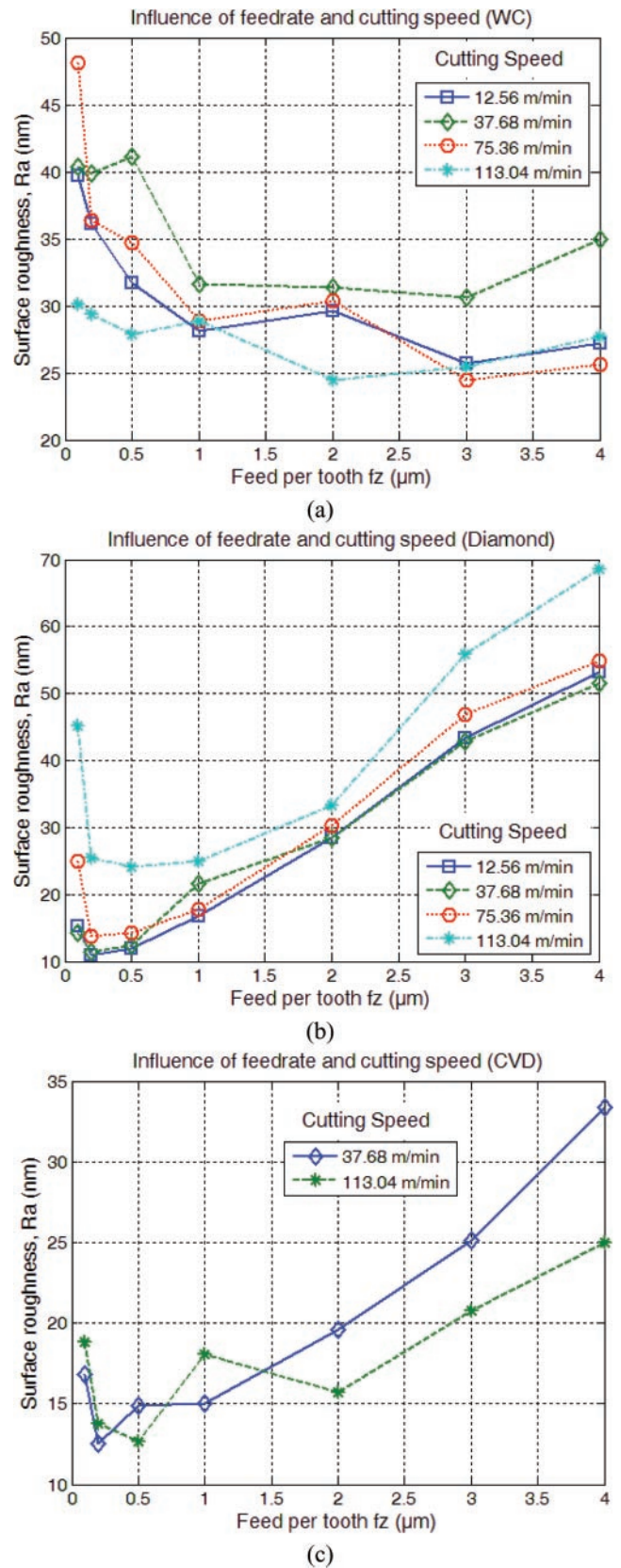

Fig. 5 Average surface roughness R_a as a function of feedrate and cutting speed: (a) WC tool; (b) single-crystal diamond tool; (c) CVD diamond tool

from a small ratio of chip thickness to tool edge radius will be a dominant factor for the material removal mechanism and chip generation physics in micromachining. Cutting, ploughing, or slipping phenomena will occur, predominated by this ratio, and will eventually influence machining processes such as surface roughness and burr formation. In previous ultra-precision machining studies, numerous researchers have investigated this size effect, and the critical minimum chip thickness was reported to be around 10–40 per cent of cutting edge radius [**5**, **27–30**]. WC micro tools used in this work have a cutting edge radius in the range of 3–6 μm measured by a scanning election microscope (SEM) for the same batch of micro tools, whereas CVD diamond and single-crystal diamond micro tools have a cutting edge radius of 0.2 μm as quoted by the manufacturer. The minimum chip thickness can well be used to explain that there exists an optimum feedrate at which micromilling produces the best surface roughness, as discussed above.

Compared with two-fluted WC micro tools, CVD and single-crystal diamond tools with one sharp cutting edge are prone to instability, because there is always either only one single cutting edge in contact with the workpiece or no contact with the workpiece, which causes periodic variation of the cutting force and poor surface roughness. For diamond micromilling, surface roughness increases sharply with feedrate when the feedrate exceeds 0.5 μm/tooth (see Fig. 5(b)), indicating that good surface roughness can only be achieved in diamond micromilling over a limited feedrate range (0.2–1.0 μm/tooth). By contrast, good surface roughness was achieved from a wider feedrate range in the WC micro tools experiments.

Figure 6 shows average surface roughness R_a as a function of axial depth of cut. Compared with the effect of feedrate on the surface roughness, there were no substantial differences for all three types of micromilling tool – surface roughness R_a increased slightly with axial depth of cut. Under the same feedrate and cutting speed, the R_a value for the deepest cut (100 μm) was just slightly higher than that for the shallowest cut (10 μm). Therefore, using a larger axial depth of cut is an effective way of increasing the machining efficiency, assuming that tool breakage and wear are not issues.

3.2 Burr formation

Burrs in micromachining can be categorized in a number of ways. According to their position, burrs can be classified as entrance, exit, top, and bottom burrs. Burrs in micromachining can be classified into four types of burr according to their shape and amount: primary burr, needle-like burr, feathery burr, and minor burr [**31**]. Sizes of entrance and exit burrs were
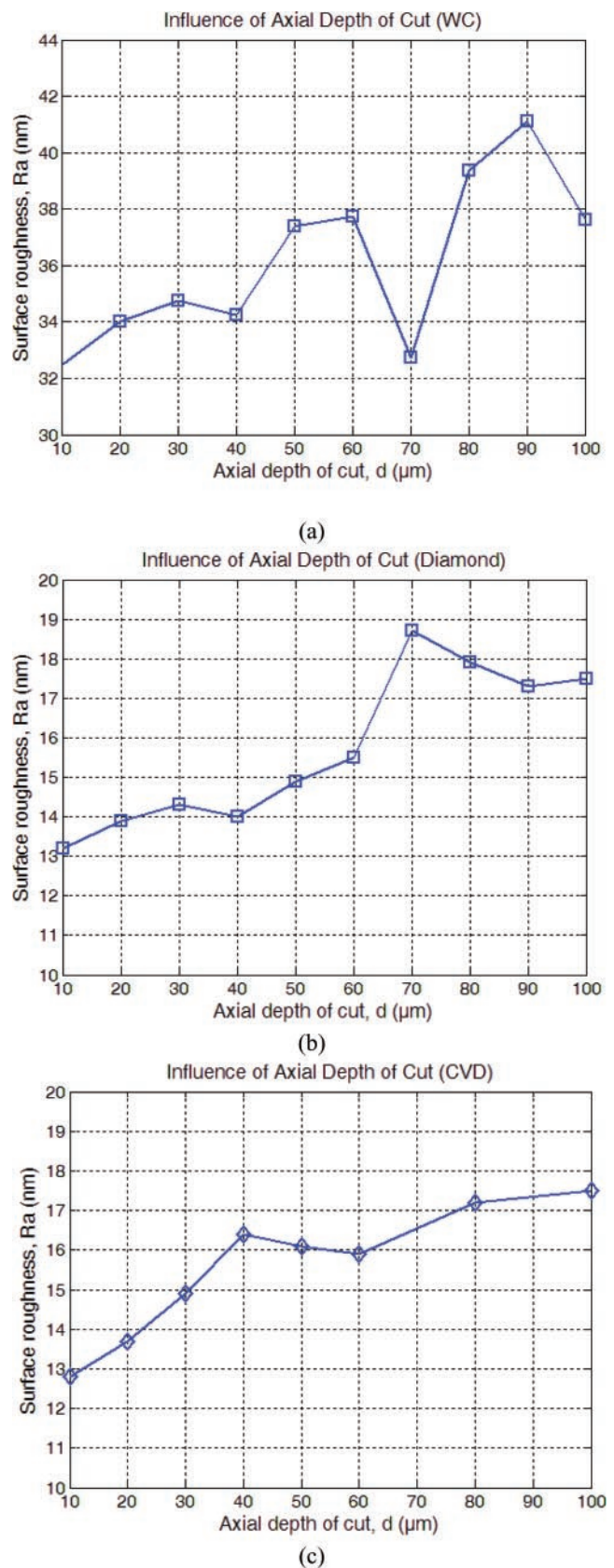

Fig. 6 Average surface roughness R_a as a function of axial depth of cut: (a) WC tool; (b) single-crystal diamond tool; (c) CVD diamond tool

found to be small, and bottom burrs were ignorable in this work. Top burrs were observed and measured in this work. Because the top burrs in this work were uniform minor burrs, average burr heights measured across the slot were used quantitatively to investigate the relationship between cutting conditions and burr formation. Figure 7 shows some examples of burr formation using diamond and WC cutters.

Burr height at various feedrates and cutting speeds is plotted in Fig. 8, and its variation with axial depth of cut is plotted in Fig. 9. In general, the relationship between burr height and cutting conditions was
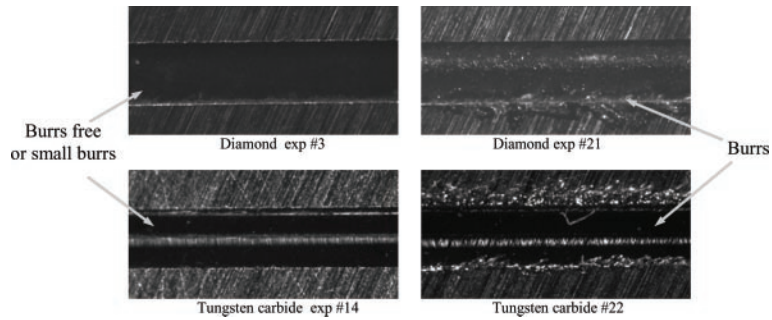

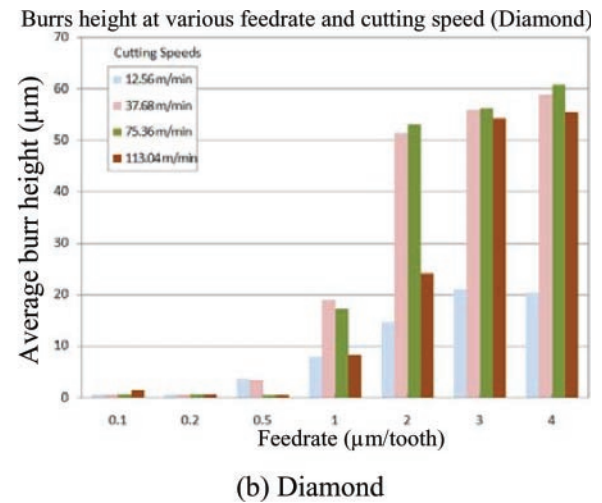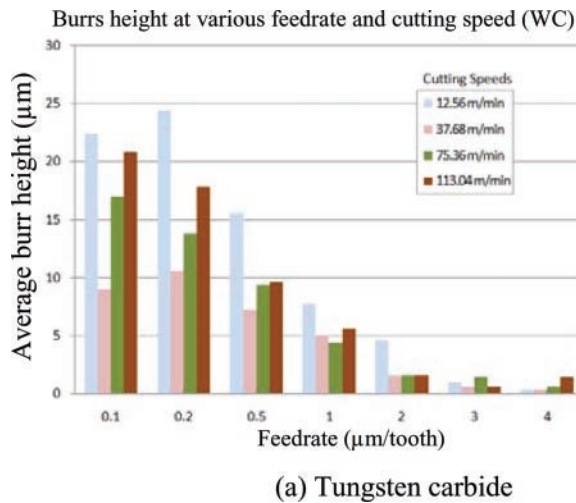**Fig. 7** Examples of burr formation for diamond and WC cutters

Fig. 8 Burr height at various feedrates and cutting speeds: (a) WC; (b) diamond
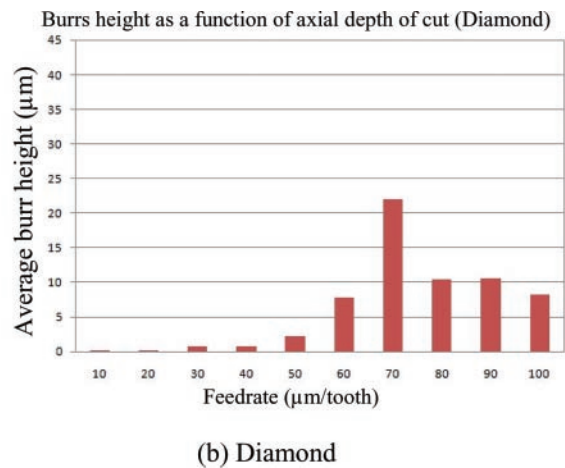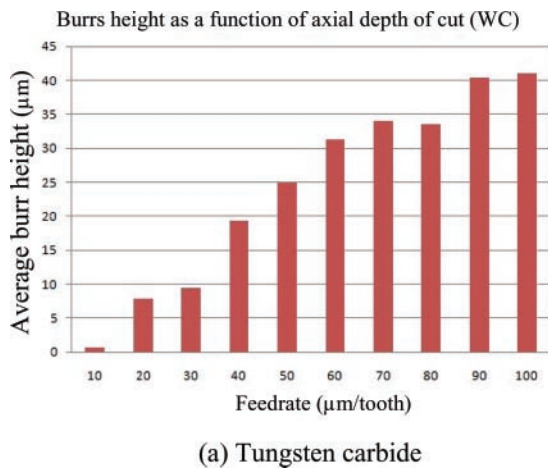

Fig. 9 Burr height as a function of axial depth of cut: (a) WC; (b) diamond

observed to be similar to that between surface roughness and cutting conditions. When the axial depth of cut is 30 μm, burr-free or small-burr-height (< 5 μm) cutting was found at a feedrate range of less than 0.5 μm/tooth for diamond tools and a feedrate range of 1–4 μm/tooth for WC micro tools, respectively (see Fig. 8). Good surface roughness normally corresponds to small top burr height for both diamond and WC micro tools, which makes cutting parameter optimization less complex. With an increase in the axial depth of cut, for the diamond and WC tools, the burr height tends to increase (see Fig. 9). Cutting speed was found to have no significant effect on burr height. However, for WC tools a medium cutting speed (37.68 m/min) produces fewest burrs, and for diamond tools a high cutting speed (113.04 m/min) helps to reduce burr formation, although more experimental data are needed further to verify this finding.

4 CONCLUSIONS AND FUTURE WORK

This paper presents an experimental investigation of micromilling OFHC copper on an ultra-precision micromilling machine. Tungsten carbide, CVD, and single-crystal diamond micro end-mills with 0.4 mm diameter were used to create full-width slots. Various cutting conditions, including feedrate, spindle speed, and axial depth of cut, were experimentally investigated, particularly in their influence on surface roughness and burr formation. The following major conclusions can be drawn from this work.

1. In micromilling using those three types of cutter, feedrate has a significant influence on surface roughness and burr height, whereas spindle speed has a slight influence on the surface roughness and burr formation. Axial depth of cut has no significant influence on the surface roughness; therefore, using a larger axial depth of cut is an effective way to increase machining efficiency.
2. The existence of the minimum chip thickness dominates the chip and surface formation at a certain feedrate range and determines the optimum feedrate and achievable surface roughness.
3. The micromilling experiments demonstrate that, if 0.4 mm diameter micro tools are used, the achievable surface roughness R_a can reach approximately 10 nm for CVD and single-crystal diamond micromilling tools and 24 nm for commercial WC micro tools through careful selection of machining conditions and the use of precision micromilling machines. The experimental results in this work provide practical and industrially feasible micromilling data using CVD and single-crystal diamond micromilling tools on precision micromilling machines.

Future efforts will be directed towards using wider cutting conditions and systematic modelling of the micromilling process based on more comprehensive cutting trial data.

REFERENCES

1 **Ehmann, K. F., Bourell, D., Culpepper, M. L., Hodgson, T. J., Kurfess, T. R., Madou, M., Rajurkar, K.,** and **DeVor, R. E.** International assessment of research and development in micromanufacturing, World Technology Evaluation Center, Baltimore, Maryland, 2005.
2 **Huo, D., Cheng, K.,** and **Wardle, F.** Design of a 5-axis ultraprecision micromilling machine – UltraMill: part 1: holistic design approach, design considerations, specifications. *Int. J. Advd Mfg Technol.*, 2009. DOI: 10.1007/s00170-009-2128-2.
3 **Huo, D., Cheng, K.,** and **Wardle, F.** Design of a 5-axis ultraprecision micromilling machine – UltraMill: part 2: integrated dynamic modelling, design optimization and analysis. *Int. J. Advd Mfg Technol.*, 2009. DOI: 10.1007/s00170-009-2129-1.
4 **Friedrich, C. R.** and **Vasile, M. J.** Development of micromilling process for high-aspect-ratio microstructure. *J. Microelectromechanical Syst.*, 1996, **5**, 33–38.
5 **Weule, H., Hüntrup, V.,** and **Tritschler, H.** Microcutting of steel to meet new requirements in miniaturization. *Ann. CIRP*, 2001, **50**(1), 61–64.
6 **Takeuchi, Y., Suzukawa, H., Kawai, T.,** and **Sakaida, Y.** Creation of ultraprecision microstructures with high aspect ratio. *Ann. CIRP*, 2006, **56**(1), 107–110.
7 **Weck, M., Hennig, J.,** and **Hilbing, R.** Precision cutting processes for manufacturing of optical components. *Proc. SPIE*, 2001, **4440**, 145–151.
8 **Liu, X., DeVor, R. E., Kapoor, S. G.,** and **Ehmann, K. F.** The mechanics of machining at the microscale: Assessment of the current state of the science. *Trans. ASME, J. Mfg Sci. Engng*, 2004, **126**(4), 666–678.
9 **Brinksmeier, E., Riemer, O.,** and **Stern, R.** Machining of precision parts and microstructures. In Proceedings of the 10th International Conference on *Precision engineering* (ICPE), *initiatives of precision engineering at the beginning of a millennium*, Yokohama, Japan, 18–20 July 2001, S. 3–11.

10 **Damazo, B. N., Davies, M. A., Dutterer, B. S.,** and **Kennedy, M. D.** A summary of micromilling studies. In proceedings of the First International Conference and General Meeting of the European Society of Precision Engineering and Nanotechnology, Bremen, Germany, 31 May–4 June 1999, pp. 322–325.

11 **Bissacco, G., Hansen, H. N.,** and **Chiffre, L. D.** Micromilling of harded tool steel for mould making applications. *J. Mater. Proc. Technol.*, 2005, **167**, 201–207.

12 **Huo, D.** and **Cheng, K.** A dynamics-driven approach to precision machines design for micro-manufacturing and its implementation perspectives. *Proc. IMechE, Part B: J. Engineering Manufacture*, 2008, **222**(B1), 1–8. DOI: 10.1243/09544054JEM839.

13 **Sweatt, W. C., Gill, D. D., Adams, D. P., Vasile, M. J.,** and **Claudet, A. A.** Diamond milling of micro-optics. *IEEE A&E Syst. Mag.*, 2008, Jan, 13–17.

14 **Chae, J., Park, S. S.,** and **Freiheit, T.** Investigation of micro-cutting operations. *Int. J. Mach. Tools Mf.*, 2006, **46**(3–4), 313–332.

15 **Rahman, M., Kumar, A. S.,** and **Prakash, J. R. S.** Micromilling of pure copper. *J. Mater. Proc. Technol.*, 2001, **116**, 39–43.

16 **Vogler, M. P., DeVor, R. E.,** and **Kapoor, S. G.** On the modeling and analysis of machining performance in micro-endmilling, Part I: surface generation. *Trans. ASME, J. Mfg Sci. Engng*, 2004, **126**, 685–694.

17 **Vogler, M. P., DeVor, R. E.,** and **Kapoor, S. G.** On the modeling and analysis of machining performance in micro-endmilling, Part II: cutting force prediction. *Trans. ASME, J. Mfg Sci. Engng*, 2004, **126**, 695–705.

18 **Kim, C. J., Mayor, J. R.,** and **Ni, J.** A static model of chip formation in microscale milling. *Trans. ASME, J. Mfg Sci. Engng*, 2004, **126**, 710–718.

19 **Lai, X., Li, H., Li, C., Lin, Z.,** and **Ni, J.** Modelling and analysis of micro scale milling considering size effect, micro cutter edge radius and minimum chip thickness. *Int. J. Mach. Tools Mf.*, 2008, **48**, 1–14.

20 **Rusnaldy, X., Ko, T. J.,** and **Kim, H. S.** Micro-end-milling of single-crystal silicon. *Int. J. Mach. Tools Mf.*, 2007, **47**(14), 2111–2119.

21 **Torres, C. D., Heaney, P. J., Sumant, A. V., Hamilton, M. A., Carpick, R. W.,** and **Pfefferkorn, F. E.** Analyzing the performance of diamond-coated micro end mills. *Int. J. Mach. Tools Mf.*, 2009, **49**(7–8), 599–612.

22 **Kussul, E., Baidyk, T., Ruiz-Huerta, L., Caballero-Ruiz, A., Velasco, G.,** and **Kasatkina, L.** Development of micromachine tool prototypes for microfactories. *J. Micromech. Microengng*, 2002, **12**(6), 795–812.

23 **Vogler, M. P., Liu, X., Kapoor, S. G., Devor, R. E.,** and **Ehmann, K. F.** Development of meso-scale machine tool (MMT) systems. *Society of Manufacturing Engineers*, 2002, Paper MS02–181, 1–9.

24 **Bang, Y. B., Lee, K. M.,** and **Oh, S.** 5-axis micromilling machine for machining micro parts. *Int. J. Advd Mfg Technol.*, 2005, **25**, 888–894.

25 **Lee, S. W., Mayor, R.,** and **Ni, J.** Dynamic analysis of a mesoscale machine tool. *Trans. ASME: J. Mfg Sci. Engng*, 2006, **128**(1), 194–203.

26 **Li, H., Lai, X., Li, C., Lin, Z., Miao, J.,** and **Ni, J.** Development of meso-scale milling machine tool and its performance analysis. *Frontiers Mech. Engng China*, 2008, **3**(1), 59–65.

27 **Filiz, S., Conley, C. M., Wasserman, M. B.,** and **Ozdoganlar, O. B.** An experimental investigation of micro-machinability of copper 101 using tungsten carbide micro-endmills. *Int. J. Mach. Tools Mf*, 2007, **47**(7–8), 1088–1100.

28 **Ikawa, N., Shimada, S.,** and **Tanaka, H.** Minimum thickness of cut in micromachining. *Nanotechnology*, 1992, **3**, 6–9.

29 **Ikawa, N., Donaldson, R. R., Komanduri, R., König, W., Aachen, T. H., McKeown, P. A., Moriwaki, T.,** and **Stowers, I. F.** Ultra-precision metal cutting – the past, the present and the future. *Ann. CIRP*, 1991, **40**(2), 587–594.

30 **Yuan, Z. J., Zhou, M.,** and **Dong, S.** Effect of diamond tool sharpness on minimum cutting thickness and cutting surface integrity in ultra-precision machining. *J. Mater. Proc. Technol.*, 1996, **62**, 327–330.

31 **Chern, G. L., Wu, Y. J. E., Cheng, J. C.,** and **Yao, J. C.** Study on burr formation in micro-machining using micro-tools fabricated by micro-EDM. *Precis. Engng*, 2007, **31**, 122–129.

JEM1828SC

Proc. IMechE Vol. 224 Part B: J. Engineering Manufacture